# Completed Hardware Design and Controller of the Robotic Cane Using the Inverted Pendulum for Walking Assistance

Phi Van Lam
School of Electrical and Computer Engineering
Yokohama National Uiversity
Yokohama, Japan 240-8501
Email: phi-lam-pv@ynu.jp

Yasutaka Fujimoto
School of Electrical and Computer Engineering
Yokohama National Uiversity
Yokohama, Japan 240-8501
Email: fujimoto@ynu.ac.jp

***Abstract*—In this paper, we propose a completed hardware design for the robotic cane, which was only demonstrated by simulation in [1], and stops as an idea in [2]. Besides, the controller of the robotic cane is verified by good experiment results like very small variations of the angle of the robotic cane, the robotic cane can stand in balance without any external forces, and it responds fast to external forces from users to return the balance point. To design the controller, the Lie Algebra (LA) method is used to linearize the nonlinear system of the inverted pendulum and find the control parameters. Besides, the Linear Quadratic Regulator (LQR) method is applied to the robotic cane to prove that the performance of LA method is better.**

## I. Introduction

Injured, elderly and disabled persons may have difficulties in standing or walking without physical assistance. In many cases, these people rely on assistive devices such as single-legged canes [8], four-legged canes, cane robot [3], and wheelchairs [7]. Further, in many cases, the user may wish to independently stand or walk a distance and minimally rely on an assistive device. Accordingly, there is an urgent requirement for researchers of new alternative devices with much more active assistance to support people to walk or stand. In this research, we realize light-weight, simplified-structure assistive devices without wearing on a body by using the inverted pendulum principle. The robotic cane using the inverted pendulum was simulated in [1]. However, the authors have not fabricated a hardware design. Thus, a completed hardware design with a fast and accurate controller is presented in this paper.

First, we present the designed hardware in section II. Next, in section III, the mathematical equations of the robotic cane are solved to find control parameters for the controller. The theories of two methods; LA method and LQR method are summarized in section IV and V. Then, the performance of the controller is proved by expriment results in section VI. Finally, we give some conclusions about applications of the robotic cane.

## II. Hardware design

A robotic cane is shown as in Fig. 1 (a) which includes a grip handle (1), a cane body (2), a balance control sensor, a center controller, and batteries (3), a motorized omnidirectional wheels coupled (4) connected to the gearbox (5). The balance control sensor provides a balance signal corresponding to an orientation of the robotic cane. The center controller receives the balance signal from the balance control sensor and calculates a balancing velocity of the motorized omnidirectional wheels based at least in part on the balance signal and an inverted pendulum control algorithm. The center controller further provides a drive signal to the motorized omnidirectional wheels in accordance with the calculated balancing velocity.

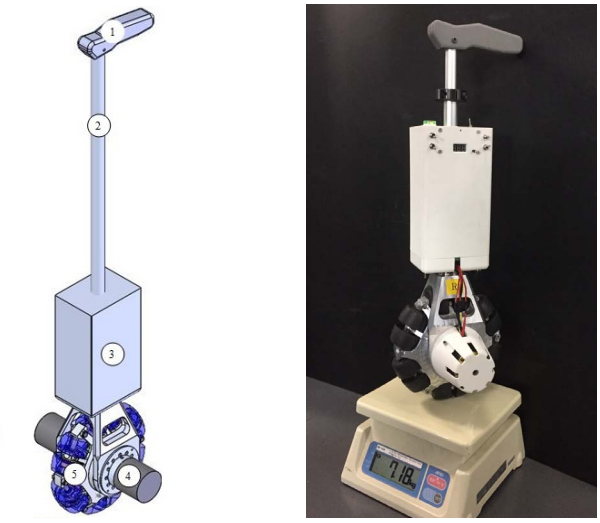


(a) Solidworks (b) Hardware

Fig. 1. Robotic cane for walking assistance

The calculated balancing velocity is a speed and direction of the motorized omnidirectional wheels to retain the robotic cane in a substantially upright position. Depending on the control signal from the algorithm in the controller, the robotic cane will stand or move.

The robotic cane moves in different directions by using two motors with omnidirectional wheels in Fig. 2. With a structure

978-1-5090-1412-5/17/$31.00 ©2017 IEEE

of harmonic gear, the robotic cane can control the speed of the big wheel more easily than other types of gearbox. Moreover, the brushless motor can create a big force for the robotic cane when users need the robotic cane to help them. We also use a high resolution encoder to detect the angle of the robotic cane when it moves. The basic operating principle of the robotic cane has four basic possibilities of motion. The robotic cane moves forwards or backward when two motors rotate clockwise or counter-clockwise. Otherwise, it moves right or moves left when two motors rotate in two different directions. Fig. 3 shows that the operating principle and structure of the minor wheels.

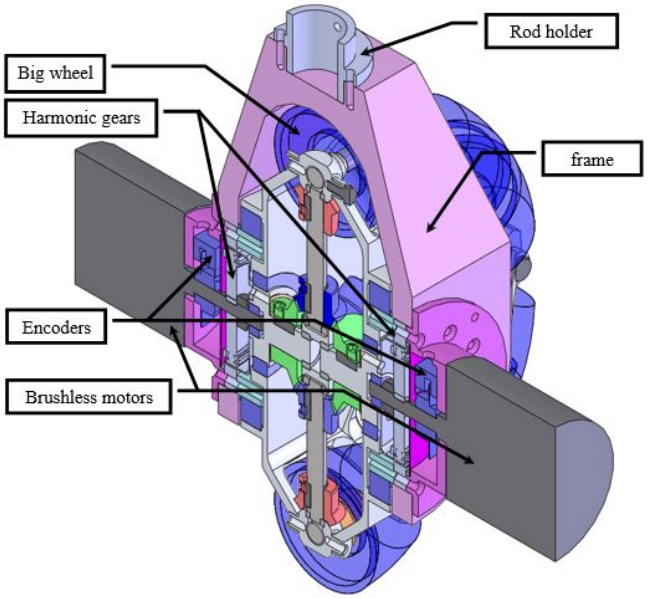


Fig. 2. The structure of the gearbox and motors

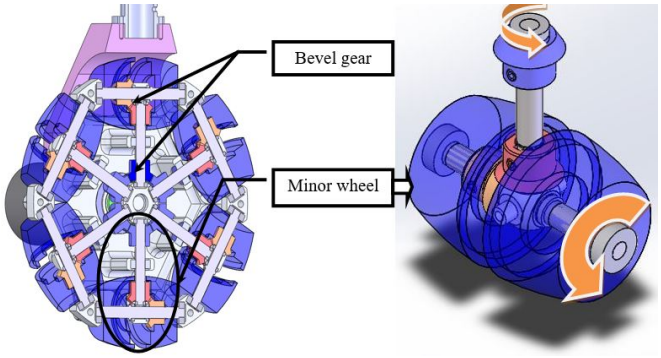


Fig. 3. Operating structure of minor wheel

By using a gyroscope sensor and accelerometer, we can detect the angle of the rod (Fig. 1) when it moves or stands. Thanks to the velocity of the robotic cane, we determine the user's force which is necessary to control the robot. Moreover, two motor drivers have been applied to the robotic cane to help it to run and control the output current for brushless motors to operate easily and perfectly. These motor drivers are controlled by received control signals from the center controller while control signals depend on the designed algorithm. The hardware of the robotic cane including the batteries is shown in Fig. 1 (b) with the weight of about 7.2 kg.

## III. Mathematical Model of the Robotic Cane

The relationship between the rotation angle of the omni-directional wheels and the rotation angle of two motors is expressed in Eq. 1 and Eq. 2. The major wheel angle, the minor wheel angle, the angle of left side motor and right-side motor are denoted $\theta_{Roll}$, $\theta_{Roll}$, $\theta_R$ and $\theta_L$, respectively.

$$\theta_{Pitch} = G\frac{\theta_R + \theta_L}{4} \tag{1}$$

$$\theta_{Roll} = G\frac{\theta_R - \theta_L}{2} \tag{2}$$

where $G$ is a ratio of the gearbox, it is designed as $G = 1/25$.

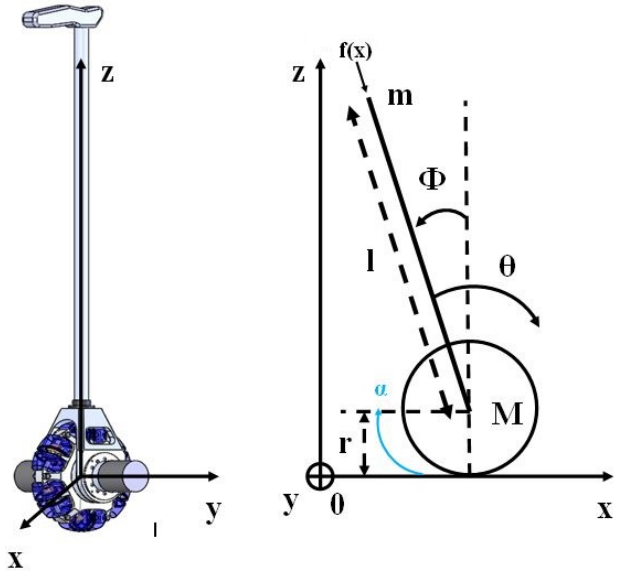


Fig. 4. Coordinate system of the robotic cane

The standard coordinate system in Fig. 4 has two basic planes: the sagittal plane - xz, and lateral plane - yz. For the sagittal plane, the robotic cane can be regarded as an inverted pendulum with a large wheel. Similarly, it can be considered as an inverted pendulum with small wheels in the lateral plane. Motion equations of the robotic cane are obtained from Lagranges equation in Eq. 3 as follows. Equations of motion in the sagittal plane and the lateral plane are the same except for their input parameters.

$$\begin{cases} \frac{d}{dt}\left(\frac{\partial L}{\partial \dot{\theta}}\right) - \frac{\partial L}{\partial \theta} + \frac{\partial \mathrm{F}_{fr}}{\partial \dot{\theta}} = \tau \\ \frac{d}{dt}\left(\frac{\partial L}{\partial \dot{\phi}}\right) - \frac{\partial L}{\partial \phi} + \frac{\partial F_{fr}}{\partial \dot{\phi}} = 0 \end{cases} \tag{3}$$

where, L is the Lagrangian.

TABLE I
EXPLANATION OF SYMBOLS

| Symbol | Explanation |
|---|---|
| $T_1$ | Rotational kinematics of Wheel |
| $T_2$ | Rotational kinematics of cane |
| $T_3$ | Translational kinematics of the wheel |
| $T_4$ | Translational kinematics of the cane |
| $T$ | Kinematics total |
| $V$ [kg·m$^3$/s] | Potential total |
| $J_\phi$ [kg·m$^2$] | Inertia of the cane |
| $J_\theta$ [kg·m$^2$] | Inertia of the wheel |
| $D_\phi$ [N.m.s/rad] | Viscous friction coefficient of cane |
| $D_\theta$ [N.m.s/rad] | Viscous friction coefficient of wheel |
| $l$ [m] | Length of the cane |
| $l_c$ [m] | Center of mass of the cane |
| $m$ [kg] | Mass of cane |
| $M$ [kg] | Mass of wheel |
| $\tau$ [N.m] | Actuation torque |
| $g$ [m$^2$/s] | Gravitational acceleration |
| $r$ [m] | Radius of the wheel |

Parameters are denoted in Table I. The state space equation of the robotic cane by using inverted pendulum model shown as Eq. 4:

$$\begin{bmatrix} H_{11} & H_{12} \\ H_{21} & H_{22} \end{bmatrix}\begin{bmatrix} \ddot{\phi} \\ \ddot{\theta} \end{bmatrix}+\begin{bmatrix} b_1 \\ b_2 \end{bmatrix}=\begin{bmatrix} 0 \\ \tau \end{bmatrix} \tag{4}$$

where, $H_{ij}$ is an element of the inertia matrix, $b_i$ is a nonlinear term expressed as follows:

$$H_{11} = J_\theta + (M+m)r^2 + 2mrl\cos\phi + J_\phi + ml^2 \tag{5}$$
$$H_{12} = H_{21} = -J_\theta - (M+m)r^2 - mrl\cos\phi \tag{6}$$
$$H_{22} = J_\theta + (M+m)r^2 \tag{7}$$
$$b_1 = -\dot{\phi}^2 mrl\sin\phi - mgl\sin\phi + D_\phi\dot{\phi} \tag{8}$$
$$b_2 = \dot{\phi}^2 mrl\sin\phi + D_\theta\dot{\theta} \tag{9}$$

From this equation, it is seen that the system of the robotic cane is a nonlinear system and nonlinear controller is based on approximate feedback linearization [6] is applied to control this system. Let $u$ be a new input. Then, the actuation torque $\tau$ is obtained as follows:

$$\tau = (H_{22} - \frac{H_{12}H_{21}}{H_{11}})u - \frac{H_{21}b_1}{H_{11}} + b_2 \tag{10}$$

In [4], [5] and [9] the authors show method to control inverted pendulum for stability around equilibrium point but focus only inverted pendulum with cart, not same with the robotic cane. In this paper, the LA method and compared with LQR method has proposed as below:

## IV. Lie Algebra method for linearization of non-linear system

Nonlinear system as the equation is shown bellow:

$$\begin{cases} \dot{x} = f(x) + g(x)u \\ y = h(x) \end{cases} \tag{11}$$

Lie Algebra method with basic equation has shown by [6] is expressed gain as follows:

$$L_f h(x) = \sum_{i=1}^{n} \frac{\partial h(x)}{\partial x} f_i(x) = \frac{\partial h(x)}{\partial x} f(x) \tag{12}$$

with the input signal $u$ is:

$$u = \frac{v - {L_f}^r h(x)}{L_g {L_f}^{r-1} h(x)} \tag{13}$$

where $v = y^{(r)}$ and:

$$v = -\sum_{i=0}^{r-1} \lambda_i (y^{(i)} - y_{ref}^{(i)}) \tag{14}$$

Return in the system, we define $y$ as a function with $\phi$ and $\theta$ as:

$$y = \int_0^\phi \frac{H_{11}}{H_{12}} d\phi + \theta \tag{15}$$
$$\dot{y} = \frac{H_{11}}{H_{12}}\dot{\phi} + \dot{\theta} \tag{16}$$
$$\ddot{y} = \frac{\partial}{\partial\phi}\frac{H_{11}}{H_{12}}\dot{\phi}^2 - \frac{b_1}{H_{12}} \tag{17}$$
$$y^{(3)} \simeq \frac{\partial^2}{\partial\phi^2}\frac{H_{11}}{H_{12}}\dot{\phi}^3 - \frac{\partial}{\partial\phi}\frac{b_1}{H_{12}}\dot{\phi} - 2(\frac{\partial}{\partial\phi}\frac{H_{11}}{H_{12}})\frac{b_1}{H_{11}}\dot{\phi} \tag{18}$$

With $r = 4$, we expand $y$ to $y^{(4)}$ by $t$ and receive two parts of input signal equation (11) as ${L_f}^4 h(x)$ and $L_g {L_f}^3 h(x)$.

## V. Linear Quadratic Regulator method

Many researchers are using LQR method as [5], [9] for the stability of the non-linear system for the inverted pendulum, but it is only linearized around the zero point while the robotic cane needs to work in a big range of the angle of the rod. Here, we use a simple approximation around $\phi = 0$, and $sin\phi \simeq \phi$, $\cos\phi \simeq 1$ and $\dot{\phi}^2\phi \simeq 0$. The Eqs. (5) to (9) should be change to Eqs. (19) to (23) as bellow:

$$H_{11} = J_\theta + (M+m)r^2 + 2mrl + J_\phi + ml^2 \tag{19}$$
$$H_{12} = H_{21} = -J_\theta - (M+m)r^2 - mrl \tag{20}$$
$$H_{22} = J_\theta + (M+m)r^2 \tag{21}$$
$$b_1 = -mgl\phi + D_\phi\dot{\phi} \tag{22}$$
$$b_2 = D_\theta\dot{\theta} \tag{23}$$

Firstly, we need to convert the above continuous state-space equations to discrete state-space, four state-space matrices (A, B, C, and D) on Eqs. (24) to (25):

$$\begin{bmatrix} \dot{\theta} \\ \ddot{\theta} \\ \dot{\phi} \\ \ddot{\phi} \end{bmatrix} = \begin{bmatrix} 0 & 1 & 0 & 0 \\ 0 & a_{22} & a_{23} & a_{24} \\ 0 & 0 & 0 & 1 \\ 0 & a_{42} & a_{43} & a_{44} \end{bmatrix}\begin{bmatrix} \theta \\ \dot{\theta} \\ \phi \\ \dot{\phi} \end{bmatrix} + \begin{bmatrix} 0 \\ b_{22} \\ 0 \\ b_{24} \end{bmatrix} u \tag{24}$$

$$y = \begin{bmatrix} 1 & 0 & 0 & 0 \\ 0 & 0 & 1 & 0 \end{bmatrix}\begin{bmatrix} \theta \\ \dot{\theta} \\ \phi \\ \dot{\phi} \end{bmatrix} + \begin{bmatrix} 0 \\ 0 \end{bmatrix} u \tag{25}$$

$$a_{22} = -\frac{H_{11}}{H_{11}H_{22} - H_{12}H_{21}} D_\theta \tag{26}$$

$$a_{23} = -\frac{H_{21}}{H_{11}H_{22} - H_{12}H_{21}} m\lg \tag{27}$$

$$a_{24} = \frac{H_{21}}{H_{11}H_{22} - H_{12}H_{21}} D_\phi \tag{28}$$

$$a_{42} = \frac{H_{12}}{H_{11}H_{22} - H_{12}H_{21}} D_\theta \tag{29}$$

$$a_{43} = -\left(\frac{H_{12}H_{21}}{H_{11}H_{22} - H_{12}H_{21}} + 1\right) \frac{m\lg}{H_{11}} \tag{30}$$

$$a_{44} = -\left(\frac{H_{12}H_{21}}{H_{11}H_{22} - H_{12}H_{21}} + 1\right) \frac{D_\phi}{H_{11}} \tag{31}$$

$$b_{22} = \frac{H_{11}}{H_{11}H_{22} - H_{12}H_{21}} \tag{32}$$

$$b_{24} = -\frac{H_{12}}{H_{11}H_{22} - H_{12}H_{21}} \tag{33}$$

The normal of feedback control law is Eq. 34, with $K$ is control matrix:

$$u = -KX \tag{34}$$

With a quadratic cost function defined as a Eq. 35:

$$J(u) = \int_0^\infty (x^T Qx + u^T Ru + 2x^T Nu)dt \tag{35}$$

The LQR method was used to find the control matrix (K). To use this LQR method, we need to find three parameters: Performance index matrix $R$ equals 1, the state cost matrix $Q$ equals of Eq. 36 and weighting factors.

$$Q = C'C \tag{36}$$

A basic schematic of the state observer of system is shown in Fig. 5:

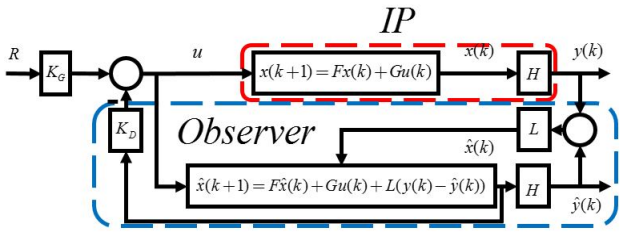


Fig. 5. The schematic controller of the LQR method

## VI. Experiment results

After finishing designing hardware of the robotic cane, we measure parameters of the robotic cane, which are given in Table II.

Next, a comparison of the working performance of two methods; LA method and LQR method is presented when they are applied to the designed hardware.

In Fig. 6, the results of the angle of the robotic cane using two methods are shown in two periods. In the first period from 0 [sec] to 50 [sec], the robotic cane balances by itself. In the last period, the robotic cane gives the feedback due to a user's force. These results show that LA method has better performance than that of the LQR traditional method.

TABLE II
Calculated parameters for experiment

| Symbol | Sagittal plane | Lateral plane |
|---|---|---|
| $T_s$ [s] | 1e-4 | 1e-4 |
| $D_\phi$ [N.m.s/rad] | 0.025 | 0.03 |
| $D_\theta$ [N.m.s/rad] | 0.025 | 0.03 |
| $l$ [m] | 0.37 | 0.445 |
| $m$ [kg] | 4.66 | 7.0 |
| $M$ [kg] | 2.60 | 0.26 |
| $g$ [m$^2$/s] | 9.80621 | 9.80621 |
| $r$ [m] | 0.1 | 0.025 |

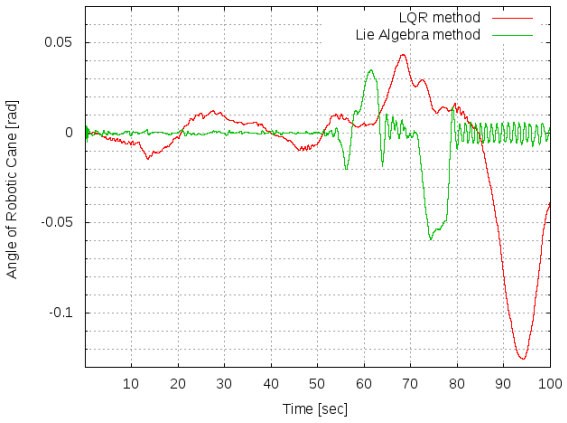


Fig. 6. The angle of robotic cane when LA method and LQR method are applied to the robotic cane

Specifically, in Fig. 7, the variation of the angle of the robotic cane when applied LA method is smaller than that of LQR method. The variation range is [−0.002[rad] : +0.002 [rad]] for LA method while the result of LQR method has the variation range of [−0.012 [rad] : +0.012 [rad]], which is 6 times bigger than that of LA method.

The better performance of LA method compared to LQR method is also shown by the result of the position of robotic cane in Fig. 8. To specify, the position of the robotic cane when LA method is applied varies from 0 [m] to 0.015 [m] while the position of the robotic cane fluctuates in 2 times bigger range from +0.005 [m] to −0.02 [m] for LQR method.

We continue considering the performances of two above methods when the robotic cane is at the equilibrium, and then, is influenced by an external force.

To LA method, in Fig. 9, at the 55th second, a force from the user is applied to the robotic cane, which changes the angle of the robotic cane suddenly. But, after only 5 seconds, the robotic cane reaches to a new equilibrium, and then, keeps balancing.

By comparison, to LQR method, when a force from the user is applied at the same time, the angle of robotic cane varies

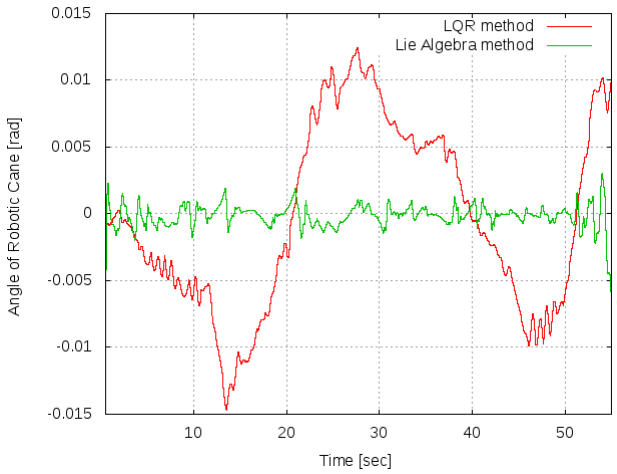


Fig. 7. Angle of the robotic cane when standing alone

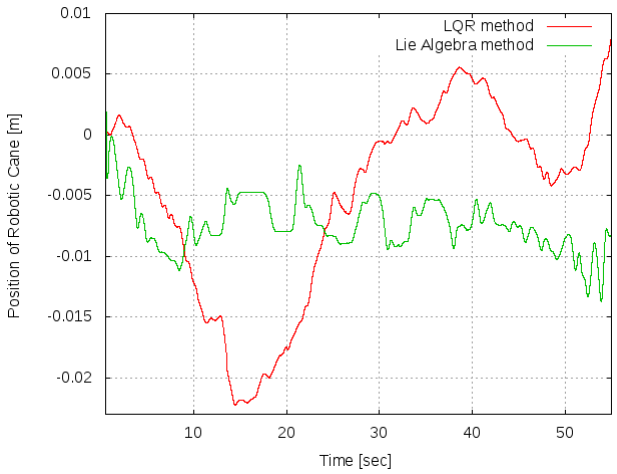


Fig. 8. Position of the robotic cane when standing alone

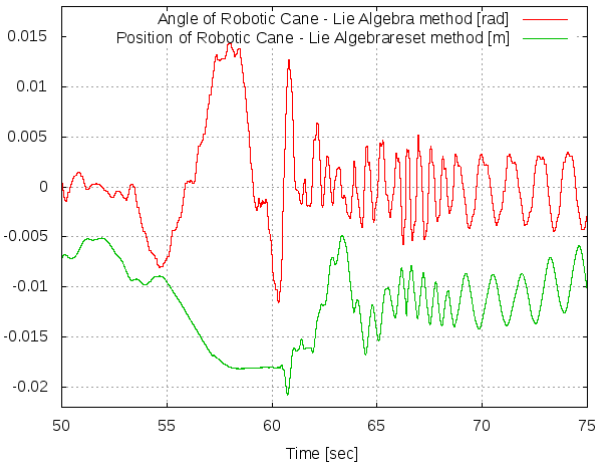


Fig. 9. Feedback of the robotic cane by the user force with the LA method

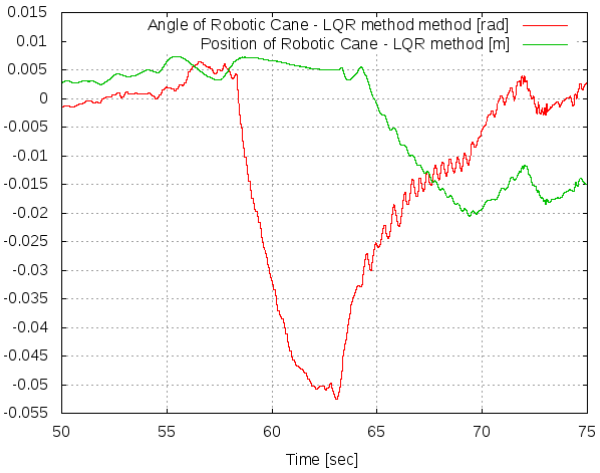


Fig. 10. Feedback of the robotic cane when an external force is applied with LQR method

from 0 [rad] to −0.054 [rad]. However, the robotic cane only gets a new equilibrium after a period of 15 seconds which is 3 times longer than that of LA method as shown in Fig. 10. This is not acceptable for applications in practice.

Next, we analyze the applicability of the LA method in the robotic cane for walking assistance as follows:

First, we test the ability of the robotic cane to balance without any external forces or support from users in Fig. 11. Here, the robotic cane has the ability to stabilize around an equilibrium over a period longer than 5 minutes with a small change its position. In this mode, the robotic cane is always ready to support users to move or stand when the users hold the handle of the robot.

In Fig. 12 (a), the results show variations of the angle of the robotic cane around equilibrium in the range of [−0.003 [rad]: +0.003 [rad]], this range is really very small so that the robotic cane can keep balanced without any big fluctuations.

In the Lateral plane, the angle of the robotic cane is similar to that in the sagittal plane, as shown in Fig. 12 (b). However, the results in Fig. 12 (a) and Fig. 12 (b) shows that the robotic cane can totally stand around the equilibrium in both planes. This verifies that the designed controller works effectively.

In the sagittal plane, in Fig. 13 (a), the result shows that the robotic cane can give necessary forces (Eq. 10) in the range of [−250 [N]: +250 [N]] on the motor axis corresponding to the movement of the robotic cane in Fig. 11, these force is converted to brushless motor drivers to control the robotic cane to move.

Moreover, comparing the results in Fig. 13 (a) with the result in Fig. 13 (b), we see that the force applied on the motor axis (Eq. 10) in the lateral plane is 20 times bigger than that in the sagittal plane because of the gear ratio of minor wheels.

Secondly, we test the performance of the robotic cane with the effect of users. Three working modes of the robotic cane are considered in this section including stand, move backward and move forward corresponding to three cases: The user goes with the robotic cane, the user tends to fall backward, and the

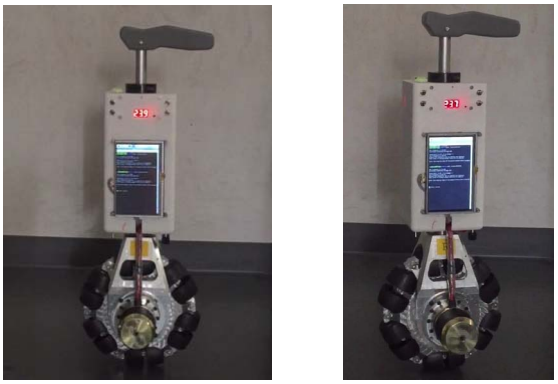

(a) Starting point (b) After 5 minutes

Fig. 11. The robotic cane standing alone

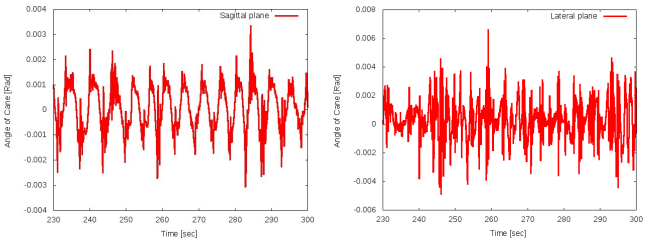


(a) Sagittal plane (b) Lateral plane

Fig. 12. The angle of robotic cane on two planes

user tends to fall forward, respectively (as shown in Fig. 14 (a), Fig. 14 (b), Fig. 14 (c), respectively).

When the robotic cane stands straight and goes with the user to support him (Fig. 14 (a)), the angle of the robotic cane is approximately zero in the first period of 10 seconds from the 20th second to around the 30th second in Fig. 14 (d); Next, when user tends to fall backward (Fig. 14 (b)), the robotic cane returns to the balanced point in next 10 seconds from the 30th to the 40th second by going backward to make the robotic cane stand in the balance. Thanks to this, the user is supported to stand straight again. Similarly, when the user tends to fall forward, the robotic cane also returns to the balanced point by moving forward. Besides, the positions of the robotic cane in three working modes are shown in Fig. 14 (e).

## VII. Conclusion

The authors successfully designed the hardware of the robotic cane using the inverted pendulum principle with the omnidirectional wheels. By linearizing the nonlinear system model of the robotic cane by LA method, the controller was also designed with the optimized control parameters. The experiment results confirmed that the robotic cane or the controller works effectively with the high processing speed and the accuracy. Therefore, the robotic cane has successfully demonstrated to be helpful as a walking assistance. Especially, the experiment results showed that the LA method works are better than LQR method.

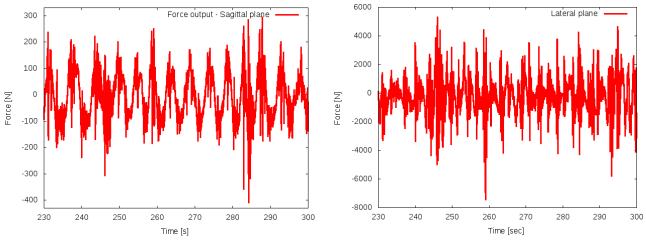


(a) Sagittal plane (b) Lateral plane

Fig. 13. Force output on motor torque of two planes

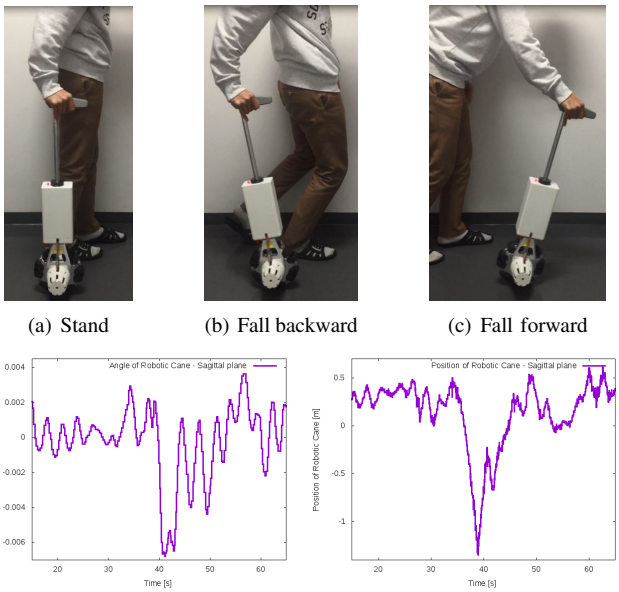


(a) Stand (b) Fall backward (c) Fall forward

(d) Angle of the robtic cane (e) Position of the robotic cane

Fig. 14. Pictures of three working modes are taken from the video while the robotic cane is working, and the appropriate angle and position of the robotic cane

## References


[1] K. Shimizu, et al., *"A Robotic Cane for Walking Support Using Two Control Modes"*, proc. IEEJ International Workshop on Sensing, Actuation, Motion Control, and Optimization (SAMCON), 2016.03.

[2] Y. Ota, et al., *"Robotic cane devices"*, US Patent Application, pub. no. US2013/0041507A1, Feb.14, 2013.

[3] S. Nakagawa, et al., *"Tandem Stance Avoidance Using Adaptive and Asymmetric Admittance Control for Fall Prevention"*, proc. IEEE Transactions on Neural Systems and Rehabilitation Engineering, (2015).

[4] J. Huang, et al., *"Nonlinear Disturbance Observer-Based Dynamic Surface Control of Mobile Wheeled Inverted Pendulum"*, proc. IEEE transactions on control systems technology, (2015).

[5] H. Fukushima, et al., *"Sliding-Mode Control for Transformation to an Inverted Pendulum Mode of A Mobile Robot With Wheel-Arms"*, proc. IEEE transactions on industrial electronic, (2015).

[6] I. A. Smad, *"Nonlinear control of mechanical systems with application to monowheel robot"*, Ph. D. thesis, Yokohama National University, 2009.

[7] C. Zhu, et al., *"A new type of omnidirectional wheelchair robot for walking support and power assistance"*, proc. IEEE/RSJ IROS, pp. 6028-6033, 2010.

[8] R. Tan, et al., *"Adaptive controller for omni-directional walker Improvement of dynamic model"*, proc. IEEE Int. Conf. on Mechatronics and Automation, pp. 325-330, 2011.

[9] R. Khairnar, et al., *"Design of Controller for Inverted Pendulum System"*, proc. International Journal of Scientific and Engineering Research, pp. 1544-1549, 2015.